

NEUTRON PROTON ELASTIC SCATTERING FROM 1 TO 6 GEV\*

M. N. Kreisler<sup>†‡</sup>, F. Martin, M. L. Perl  
Stanford University, Stanford, California

and

M. J. Longo and S. T. Powell III  
University of Michigan, Ann Arbor, Michigan

In this letter we are reporting the first high energy measurements ( 1 to 6.3 GeV kinetic energy) of neutron-proton elastic scattering extending from the small angle, diffraction peak region to the region beyond  $90^{\circ}$  in the center-of-mass system. Previous high energy measurements<sup>1, 2</sup> have only concerned elastic neutron-proton scattering near  $180^{\circ}$  in the so-called charge exchange backward peak region. This experiment was carried out at the Bevatron of the Lawrence Radiation Laboratory and used a neutron beam, spark chambers and a liquid hydrogen target. There were three objectives in this experiment:

1. To verify the existence of the expected but hitherto unobserved diffraction peak, to determine its parameters, and to investigate possible shrinkage.
2. To examine the differential cross section at and beyond  $90^{\circ}$  in the center-of-mass system, a region inaccessible in proton-proton scattering.
3. To look for the secondary forward peak which appears in pion-proton elastic scattering<sup>3, 4</sup> but not in proton-proton elastic scattering.

The experiment involved a new technique using a neutron beam containing neutrons of all energies up to 6.3 GeV kinetic energy. Neutrons, produced by

( submitted to Physical Review Letters)

the external proton beam of the Bevatron hitting a beryllium target, were formed into a beam by a 15 foot long lead collimator set at  $1^\circ$  to the proton beam direction. Bending magnets removed charged particles from the beam and lead plates reduced gamma ray contamination. From analysis of the elastic events, the neutron spectrum was found to peak at 5.0 GeV and two-thirds of the neutrons which gave events had energies above 4.0 GeV. Thus, this is a high energy beam and in fact, the spectrum was more favorable than expected.

The neutron beam with a diameter of 1.25 inches interacted in a 12 inch long hydrogen target as shown in Fig. 1. A system of thin plate spark chambers and a magnet were used to detect the recoil proton from the elastic scattering and to measure its angle and momentum. A set of seven spark chambers with 3/16 inch thick stainless steel plates was used to detect the scattered neutron by its interactions. The interaction or conversion of the neutron appeared as a neutron star of one or more prongs. The proton detecting system and the neutron detecting chambers were both on a circular rail centered on the hydrogen target. With seven different settings of their positions all scattering angles at all energies above 1 GeV were covered. The spark chambers were triggered when a set of long, horizontal, scintillation counters interspaced among the neutron chambers and two long, horizontal, scintillation counters,  $P_1$  and  $P_2$ , in the proton system indicated an approximately coplanar event had occurred.

The angle of the incident neutron was known to  $\pm 0.2$  degrees and the angle of the scattered neutron, determined by the line from the interaction point in the target to the conversion point in the neutron spark chambers was known to  $\pm 0.5$  degrees. These angles, combined with the angle and momentum of the recoil proton, overdetermined an elastic scattering, and yielded the incident neutron energy. The energy dependence of the conversion efficiency of the neutron spark

chambers was measured by setting up the apparatus for small angle scattering and triggering only with the proton system counters. At small angles the recoil proton angle and momentum was sufficient by itself to determine an elastic scattering. The fraction of events which showed neutron conversion in the neutron chambers then gave directly the conversion efficiency. This efficiency was 62 percent at 6 GeV and dropped to 45 percent at 2 GeV.

Corrections have been applied to the data for angular bias in the spark chambers, multiple scattering in the hydrogen target, small angle cutoffs, and inelastic contamination. The relative normalization between the different settings was obtained by two sets of scintillation counters which measured the scattered charged particle flux from the hydrogen target. No absolute normalization was available from the experiment itself. We have normalized the data by fitting the small angle regions with an exponential in  $t$ , the square of the four-momentum transfer from the incident to the scattered neutron, and by using the optical theorem and the neutron-proton total cross sections.<sup>5</sup> We took the real part of the forward scattering amplitude to be zero.<sup>6</sup>

For presentation we have grouped the events into ranges of incident neutron kinetic energy. The data presented is based on 6219 elastic events which represents about 15% of our available data. Figure 2 is a semi-logarithmic plot of the differential cross sections  $d\sigma/d|t|$  versus  $|t|$  [ $|t|$  is expressed in  $(\text{GeV}/c)^2$ ], and the data is shown in Table I.

In terms of the center-of-mass scattering angle  $\theta^*$  and the center-of-mass momentum  $p^*$

$$|t| = 2 p^{*2} (1 - \cos \theta^*)$$

and

$$\frac{d\sigma}{d|t|} = \pi/p^{*2} \frac{d\sigma}{d\Omega^*}$$

The cross sections as a function of  $\cos \theta^*$  were computed from  $d\sigma/d|t|$  using the average values of  $p^*$  for each incident energy range shown in Table II.

We first observe that, as expected by our general understanding of high energy elastic scattering in the presence of a large inelastic cross section, there is a strong diffraction peak at all energies. The peak has a roughly exponential behavior.

We have fit the region  $0.2 < |t| < 0.6$  (GeV/c)<sup>2</sup> with the form  $d\sigma/d|t| = A \exp(b|t|)$  and  $b$  is given in Table II. According to recent data of Clyde et al.,<sup>7</sup> the values of  $-b$  for proton-proton scattering at 2.2, 4.1, and 6.2 GeV are  $6.50 \pm 0.03$ ,  $7.44 \pm 0.04$ , and  $7.69 \pm 0.04$  (GeV/c)<sup>-2</sup>. The neutron-proton and proton-proton diffraction peak slopes have about the same values except perhaps at the lower energies. The slopes in the energy region from 2 to 6 GeV indicate a shrinkage of the diffraction peak quite similar to proton-proton scattering.

The following observations may be made on the large angle region. The differential cross section deviates from exponential and begins to flatten out as  $\theta^* = 90^\circ$  is approached. It is roughly flat, that is, isotropic near  $90^\circ$  and the minimum in the differential cross section is at or just beyond  $90^\circ$ . This isotropy near  $90^\circ$  is predicted both by the statistical model<sup>8</sup> and by the model of Wu and Yang.<sup>9</sup> Beyond  $90^\circ$   $d\sigma/d|t|$  increases even though the values of  $|t|$  are very large. This leads to the idea that  $t$  is no longer the meaningful parameter because the neutron and proton are exchanging their charges, and  $u$  (the square of four momentum transfer from the incident neutron to the recoil proton) is the relevant parameter. Since  $|u| = 4p^{*2} - |t|$ ,  $|u|$  is decreasing as  $\theta^*$  approaches  $180^\circ$ . In this experiment we used a slightly different technique to measure the region near  $180^\circ$ , but that data is not completely analyzed yet. Comparison with other data<sup>1,2</sup> near  $180^\circ$  indicates that our differential cross section will rise

roughly monotonically into the charge exchange peak. However, in the backward angle regions presented in Fig. 2,  $d[\ln(d\sigma/d|u|)]/d|u|$  is about  $0.6 \text{ (GeV/c)}^{-2}$  compared to 40 or 50  $\text{(GeV/c)}^{-2}$  at  $180^\circ$ .

The statistical model predicts an exponential decrease with the center-of-mass total energy  $W^*$  of the form  $(d\sigma/d\Omega^*)_{90^\circ} = A \exp(-gW^*)$ . We found  $g$  to be  $3.73 \pm 0.38 \text{ (GeV)}^{-1}$ . If we fit the decrease with a power of  $W^*$ , namely  $(d\sigma/d\Omega^*)_{90^\circ} = CW^{*-N}$ , then  $N = 11.04 \pm 1.15$ . Finally, Clyde et al. <sup>7</sup> give the proton-proton differential cross section at  $90^\circ$  as  $0.45 \pm 0.01$ ,  $0.016 \pm 0.0009$ , and  $0.00078 \pm 0.00004 \text{ mb/(GeV/c)}^2$  at 2.2, 4.1 and 6.2 GeV. <sup>10</sup> Interpolation of our data yields  $0.32 \pm 0.05$ ,  $0.017 \pm 0.006$  and  $0.0014 \pm 0.0008 \text{ mb/(GeV/c)}^2$  at these energies.

We find no clear evidence for a second forward peak in the neutron-proton system. There are some ambiguous indications as can be seen from Fig. 2, which should be resolved when the remainder of our data is analyzed.

We are very grateful to Mr. T. L. R. Elder, Mr. Orman Haas, Mr. James Moss, Mr. Ronald Seefred, and to the Bevatron staff for their very valuable assistance during the setup and execution of the experiment.

## FOOTNOTES AND REFERENCES

\* Supported in part by the U. S. Atomic Energy Commission and by the U. S. Office of Naval Research Contract NONR 1224 (23).

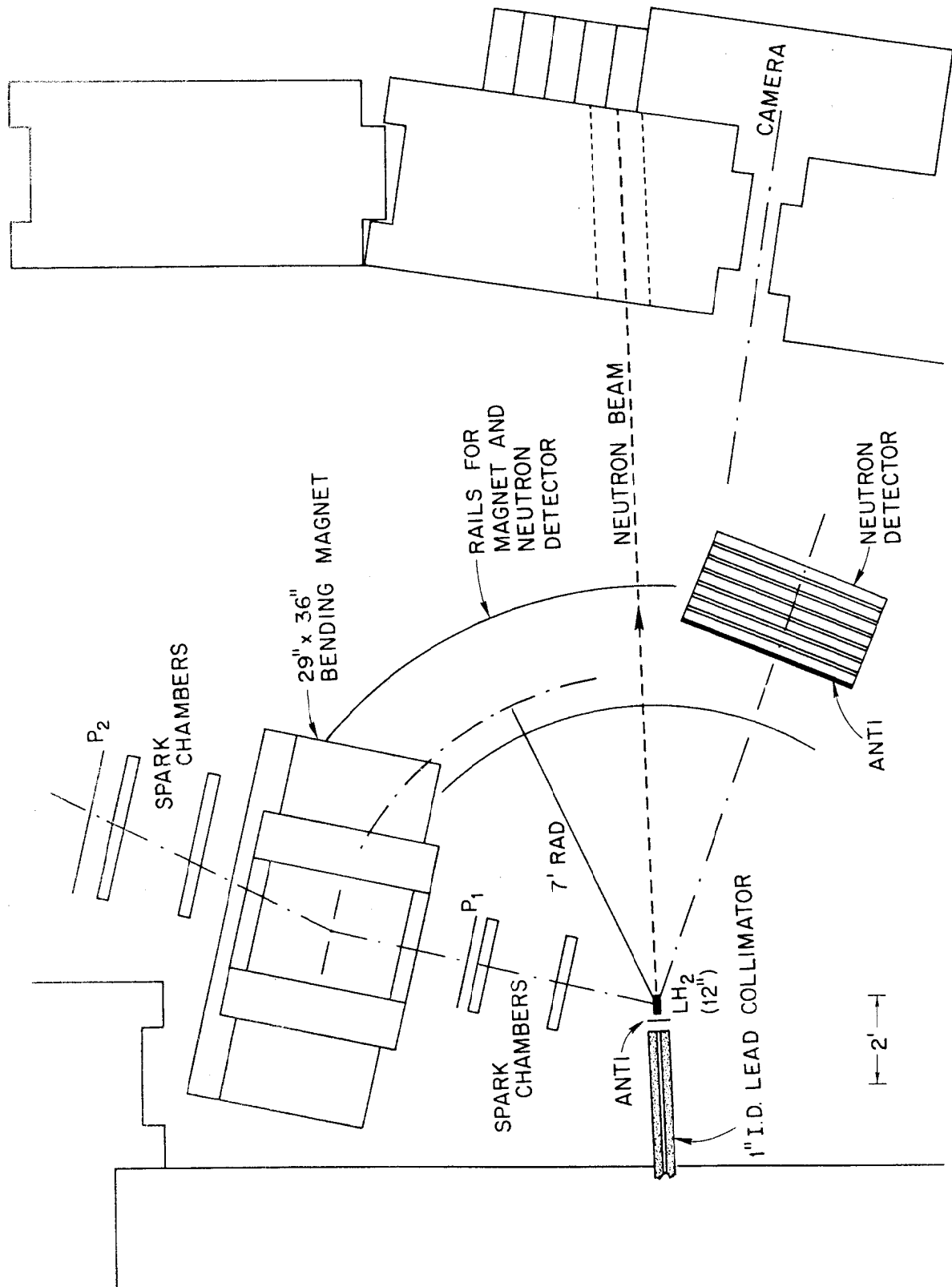
† National Science Foundation Predoctoral Fellow.

‡ This paper constitutes part of the thesis of M. N. Kreisler to be submitted in partial fulfillment of the requirements for the degree of Doctor of Philosophy, Stanford University.

1. J. L. Friedes et al., Phys. Rev. Letters 15, 38 (1965).
2. G. Manning et al., Nuovo Cimento 41, 167 (1966).
3. D. E. Damouth, L. W. Jones, and M. L. Perl, Phys. Rev. Letters 11, 287 (1963).
4. C. T. Coffin et al., Phys. Rev. Letters 15, 838 (1965).
5. D. V. Bugg et al., Rutherford Laboratory Preprint RPP/H/13, (unpublished) (1966).
6. L. Kirillova et al., abstract presented at Oxford International Conference on Elementary Particles (1965); Kh. Chernev et al., JINR-E-2413, (unpublished), (1965). The data is consistent with the real part being zero.
7. A. R. Clyde et al., UCRL 11441 (1964); A. R. Clyde (private communication).
8. G. Fast, R. Hagedorn, and L. W. Jones, Nuovo Cimento 27, 856 (1963).
9. T. T. Wu and C. N. Yang, Phys. Rev. 137, B708 (1965).
10. The 6.2 GeV value was actually at  $\theta^* = 82.3^\circ$ .

## LIST OF FIGURES

1. Layout of experimental apparatus.
2. Neutron-proton differential cross sections versus  $|t|$ .



526-1-B

Fig. 1

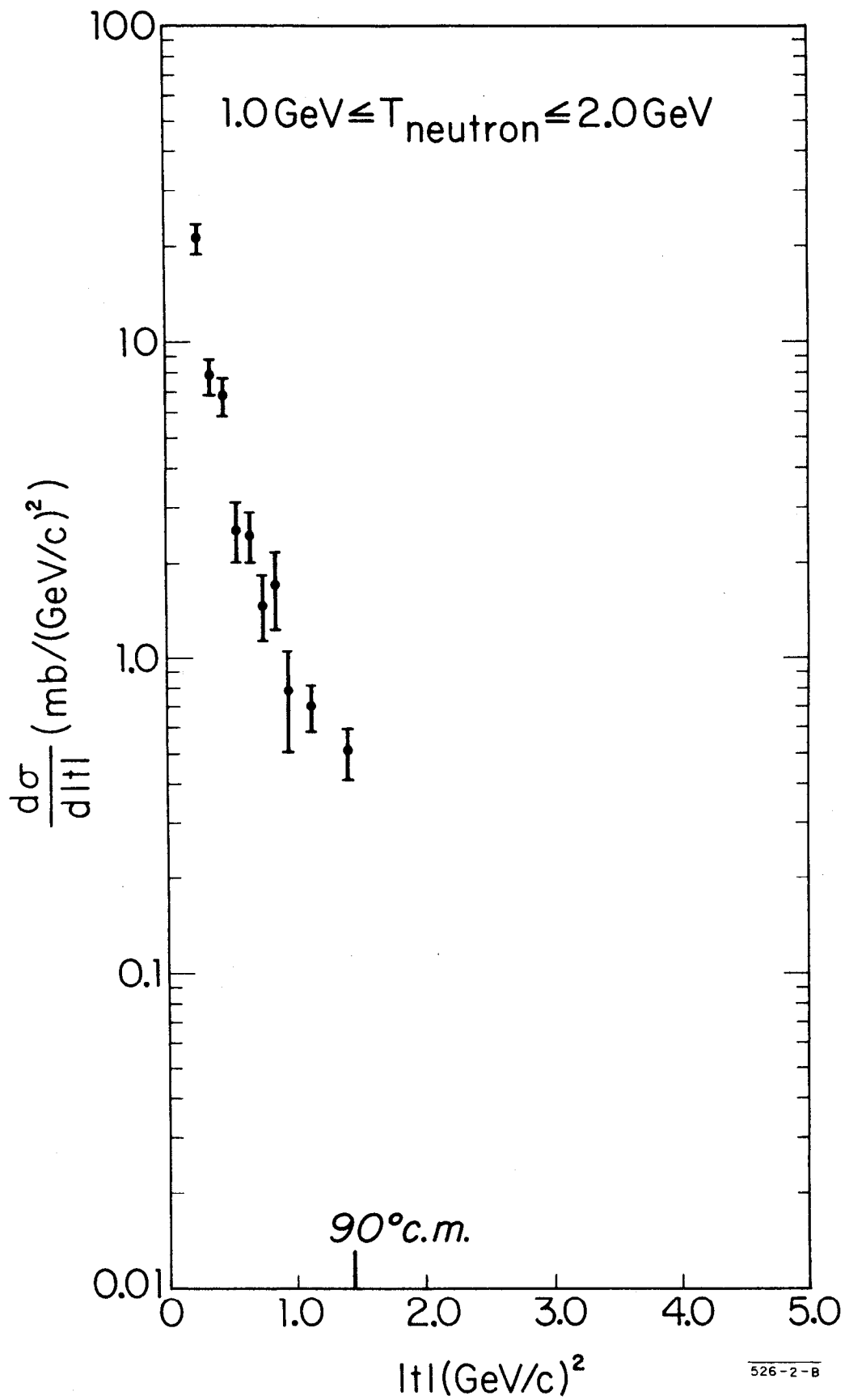


Fig. 2a

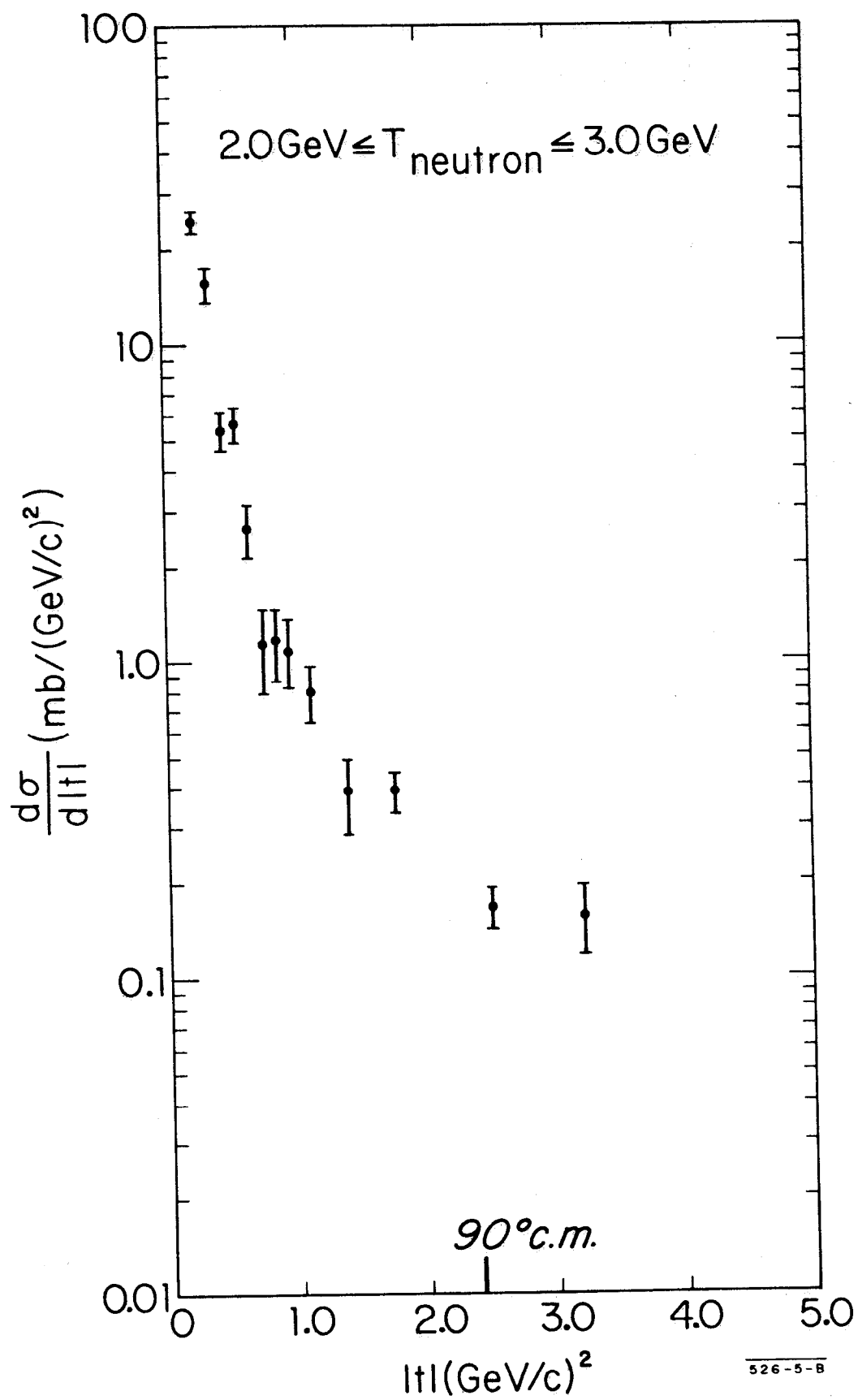


Fig. 2b

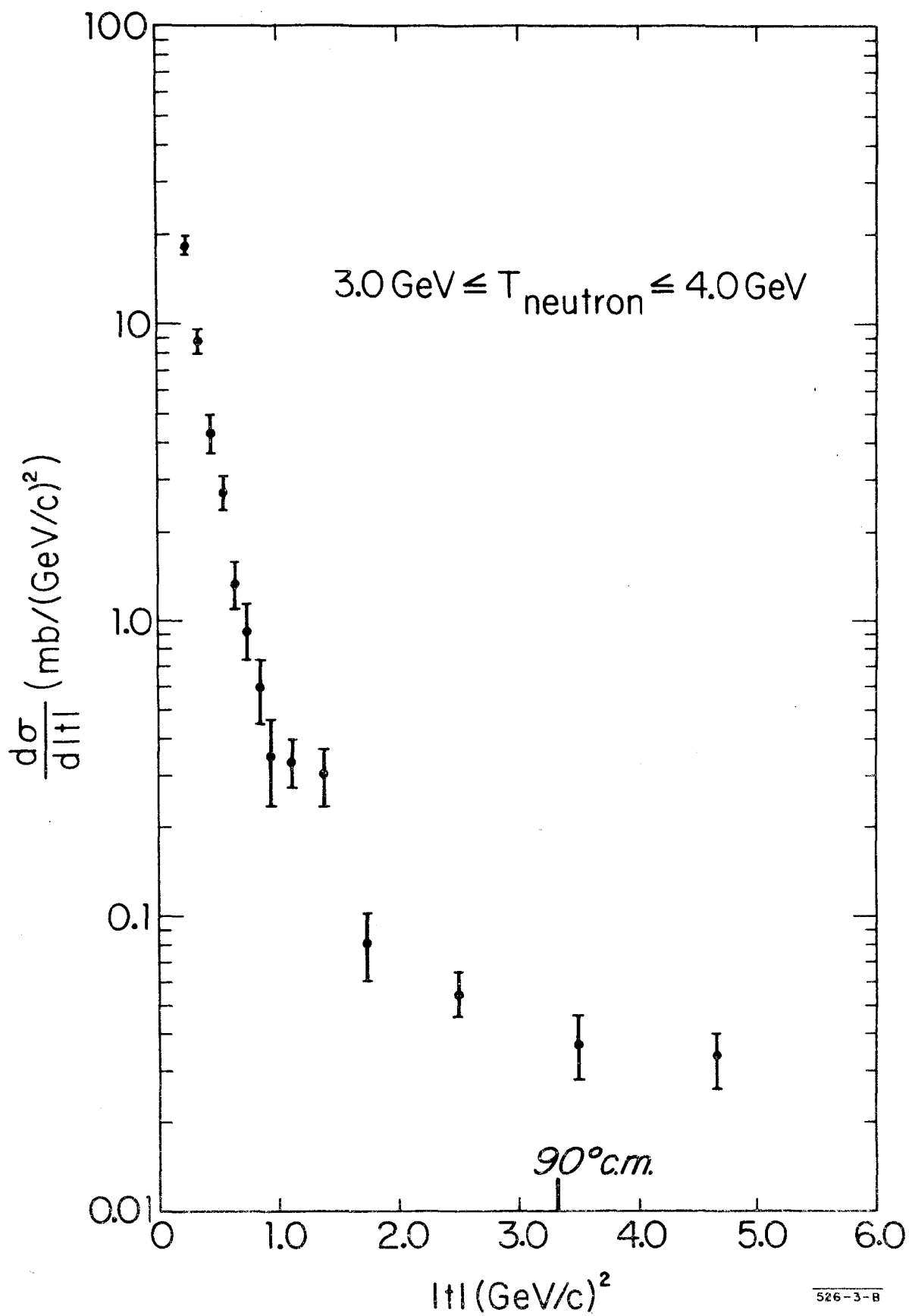


Fig. 2c

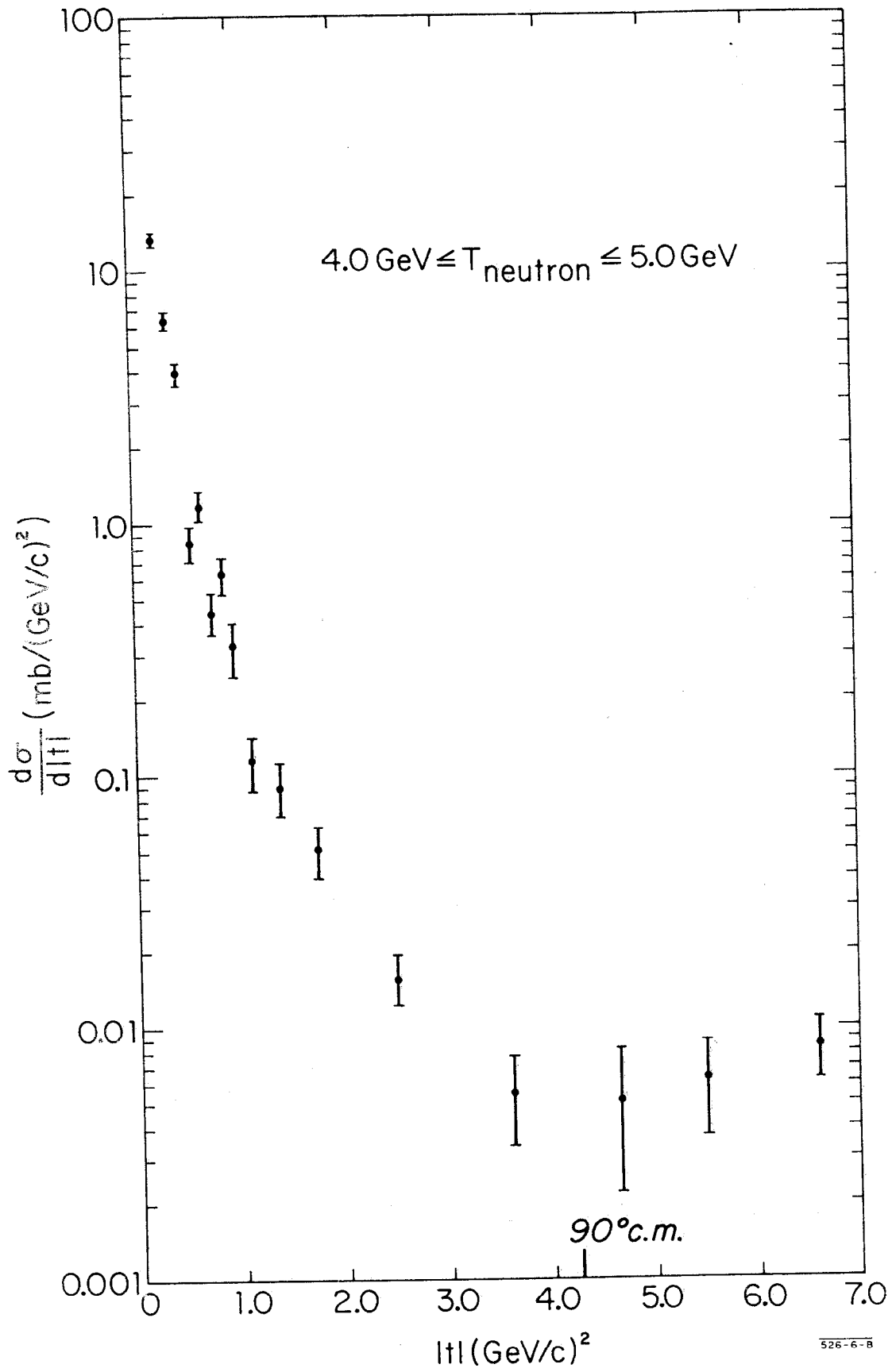


Fig. 2d

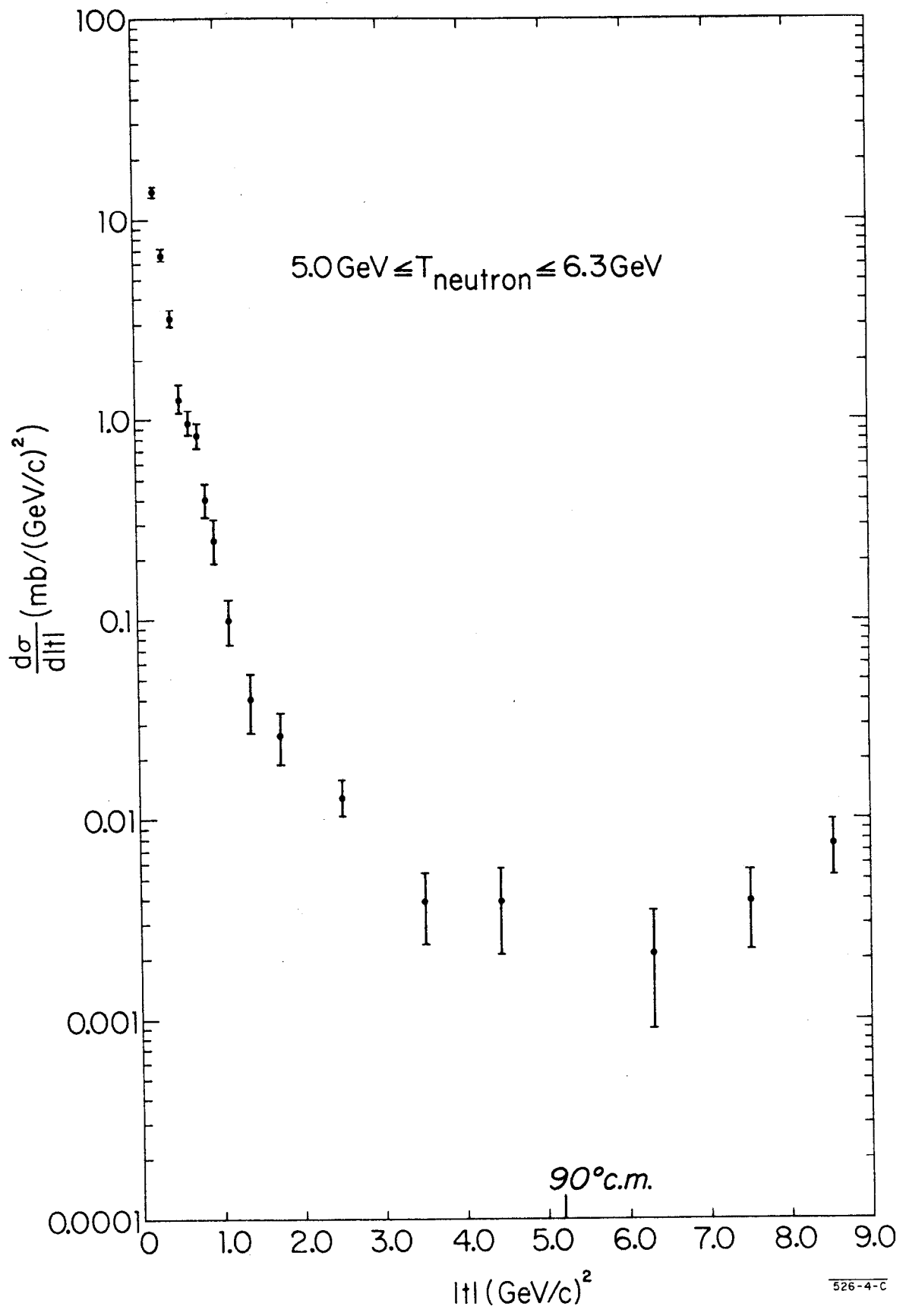


Fig. 2 e



TABLE II

Incident Kinetic Energy Range (GeV)	P* Average (Momentum in Center-Of-Mass) (GeV/c)	b (GeV/c) <sup>-2</sup>
1.0 - 2.0	0.851	- 6.321 ± 0.647
2.0 - 3.0	1.096	- 5.527 ± 0.463
3.0 - 4.0	1.287	- 6.655 ± 0.432
4.0 - 5.0	1.460	- 7.720 ± 0.411
5.0 - 6.3	1.612	- 7.562 ± 0.391